



Radiographic observation of microstructure displacement field

**Daniel Vavřík^{1,2}, Jiri Dammer², Tomáš Holý², Jan Jakůbek²,
Martin Jakůbek², Ivan Jandejsek¹**

¹ITAM AS CR, v.v.i, Prosecká 76, 190 00 Praha 9

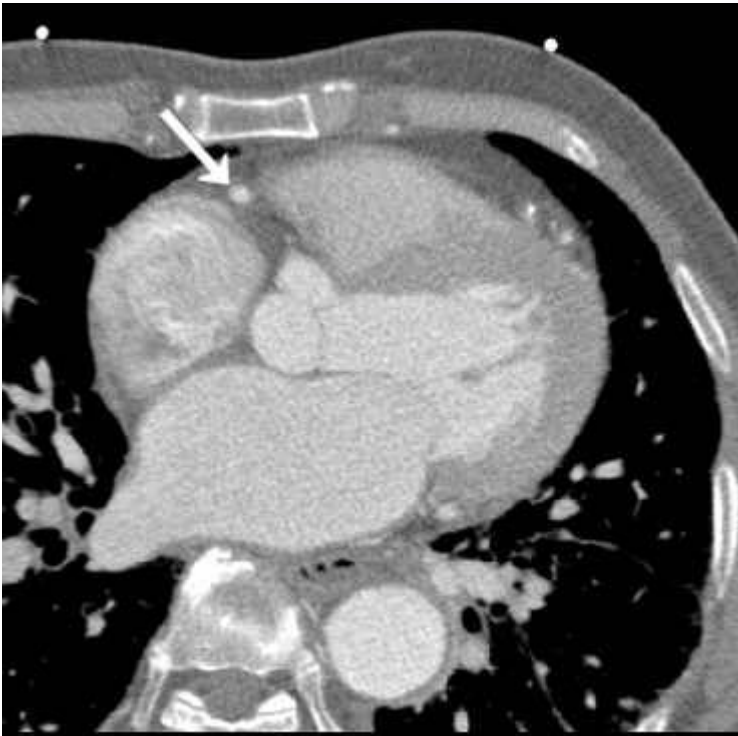
²IEAP CTU in Prague, Horská 3a, Praha 2

Motivation

- Description of the strain field in vicinity of crack tip is fundamental task for Fracture mechanics science.
- Radiography of moving objects is advanced problem when dynamic range of acquired radiograms is restricted by limited exposition time. Exposition time has to be as short as to avoid images blurring due to object moving.
- It is possible to increase dynamic range by summing of short time phase correlated radiograms when periodical object movement is presented
- Non periodical movement can be studied using tools of image correlation technique on other hand as will be shown.

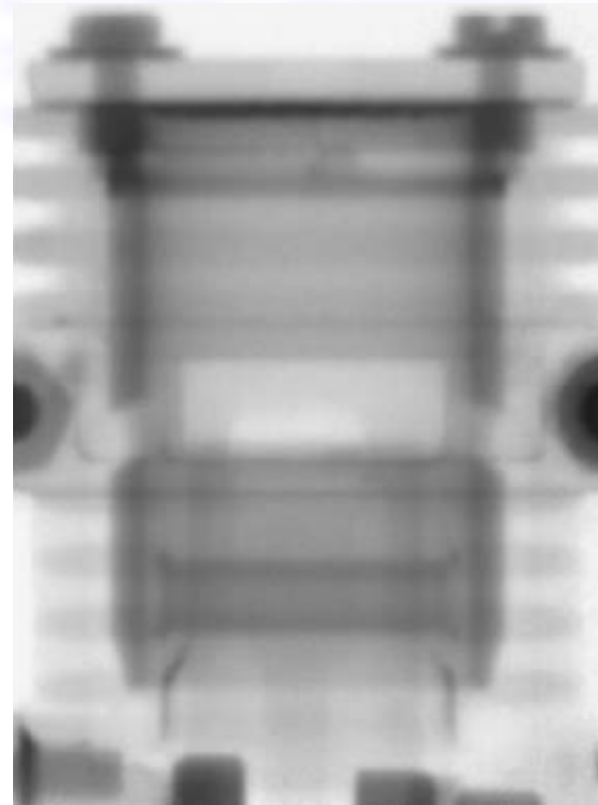
Periodic movement

ECG-Based Cardiac CT Imaging



www.imp.uni-erlangen.de

Neutron radiography of a running model aircraft engine (Sum of several 1ms radiographs).

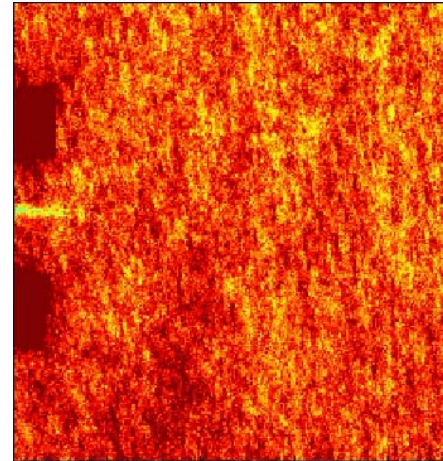


N. Kardjilov et al. / Nuclear Instruments and Methods in Physics Research A 542 20 (2005)

Non periodic motion

- Synchronization signal is not available
- Region of the interest is presented in all analyzed radiograms

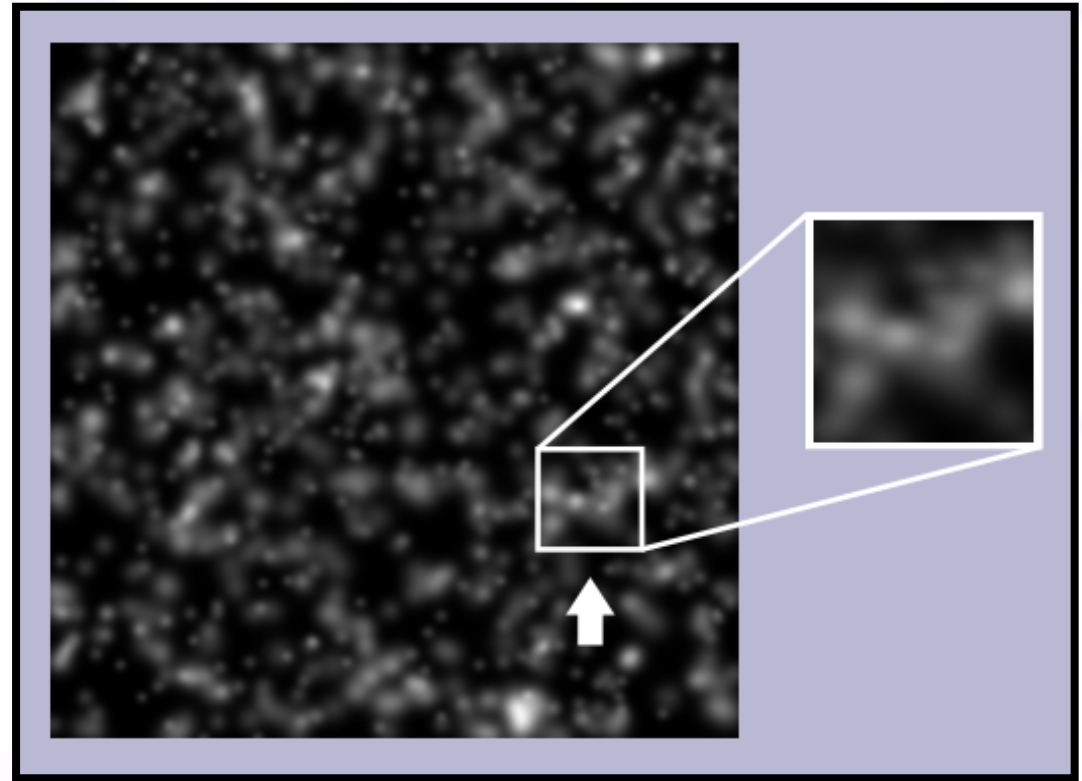
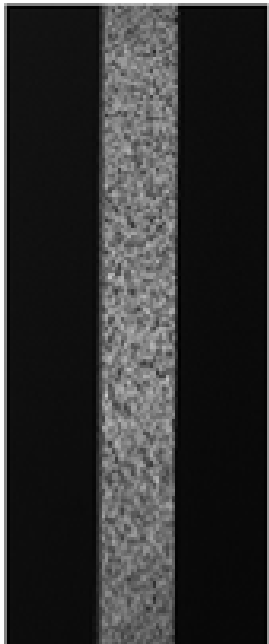
Al-alloy specimen



Radiographic observation of internal object structure X-ray Digital Image Correlation (XDIC) technique.

DIC principles for low contrast fine structures

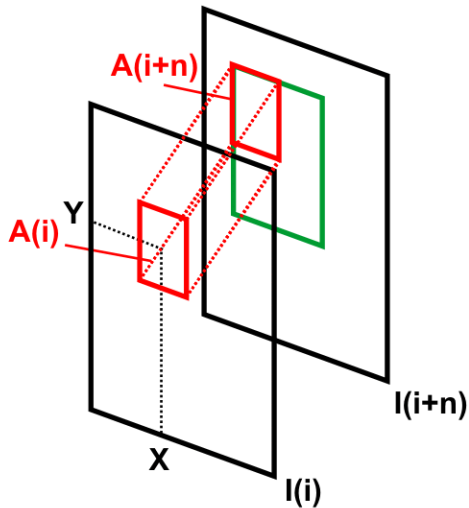
- Tracking of a pattern selected (subset) in the observed random structure



Sample

The procedure for calculation of new position of traced pattern

Target area scanned by the reference pattern

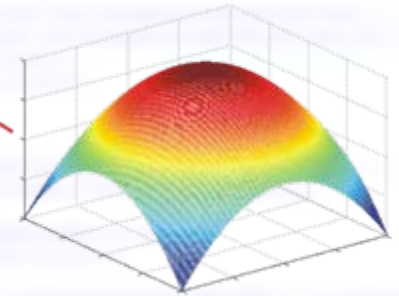


Matrix of cross correlation coefficients

0.11	0.18	0.25	0.31	0.36	0.38	0.38	0.35	0.30
0.15	0.24	0.34	0.43	0.50	0.54	0.55	0.52	0.46
0.17	0.28	0.40	0.52	0.63	0.70	0.73	0.70	0.63
0.16	0.29	0.42	0.57	0.71	0.82	0.88	0.88	0.80
0.13	0.26	0.40	0.57	0.74	0.88	0.97	0.99	0.91
0.07	0.19	0.33	0.48	0.64	0.78	0.87	0.89	0.84
0.02	0.12	0.24	0.38	0.51	0.62	0.70	0.73	0.71
-0.04	0.04	0.14	0.25	0.36	0.46	0.53	0.56	0.55
-0.06	-0.00	0.06	0.14	0.22	0.29	0.35	0.38	0.38

The matrix of cross correlation coefficients is shown. A red box highlights the peak values in the matrix, which are 0.88, 0.88, and 0.80 in the fourth row, seventh, eighth, and ninth columns respectively. A red arrow points from this peak to the interpolation surface.

Interpolation surface



The peak of interpolation surface determines a new position of the reference pattern with subpixel accuracy.

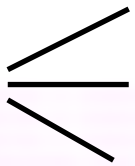
Evaluation of correspondence is based on cross correlation coefficient calculation

Cross correlation coefficient:

$$r = \frac{\sum_m \sum_n (A_{m,n}^{(1)} - \bar{A}^{(1)}) (A_{m,n}^{(2)} - \bar{A}^{(2)})}{\sqrt{\left(\sum_m \sum_n (A_{m,n}^{(1)} - \bar{A}^{(1)})^2 \right) \left(\sum_m \sum_n (A_{m,n}^{(2)} - \bar{A}^{(2)})^2 \right)}}$$

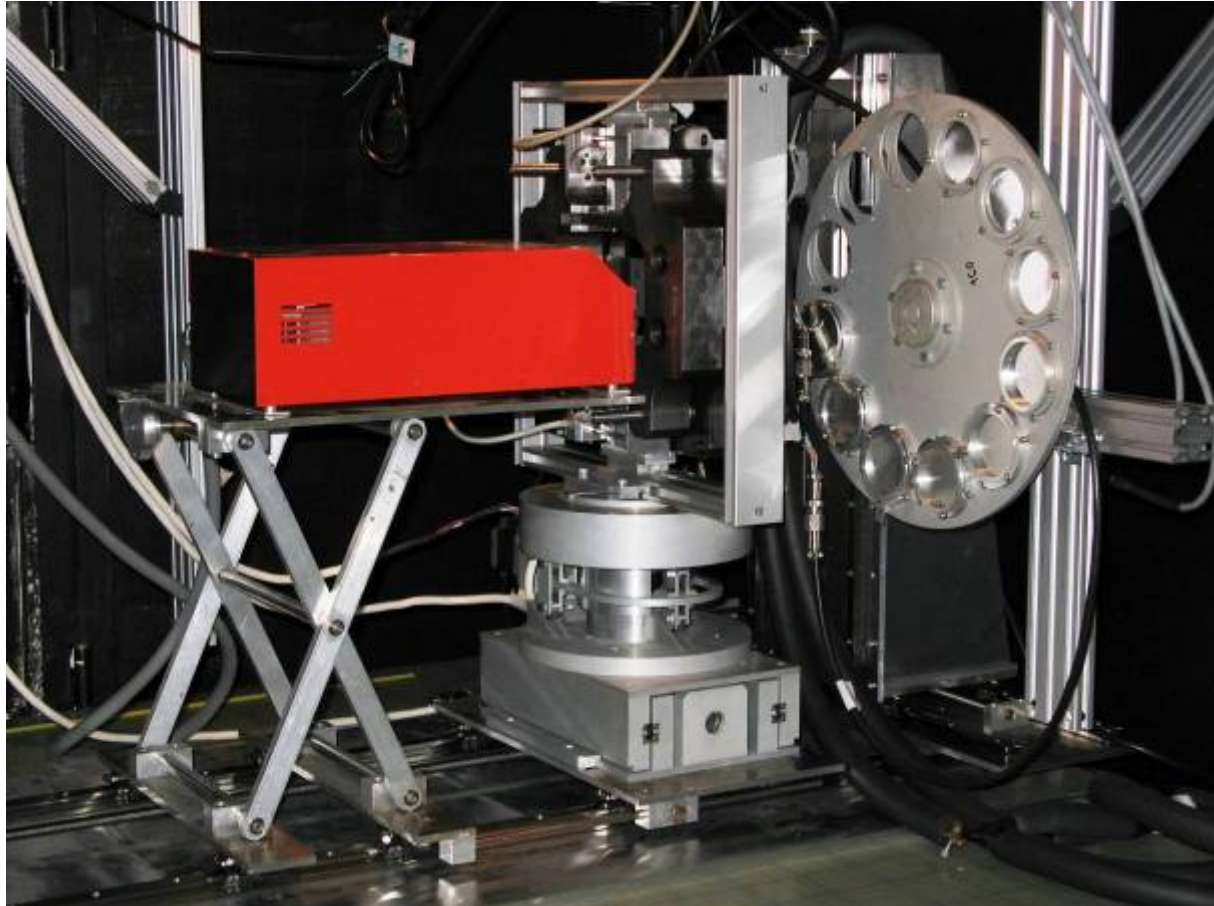
$A^{(1)}$ – Reference pattern

$A^{(2)}$ – Target pattern for which cross correlation coefficient is calculated.

$r \in \langle -1, 1 \rangle$ 

- $r = 1$... equal
- $r = 0$... indiferent
- $r = -1$... negative equal

Experimental setup



$5\mu\text{m}$ microspot X-ray tube @ 70kV, $140\mu\text{A}$

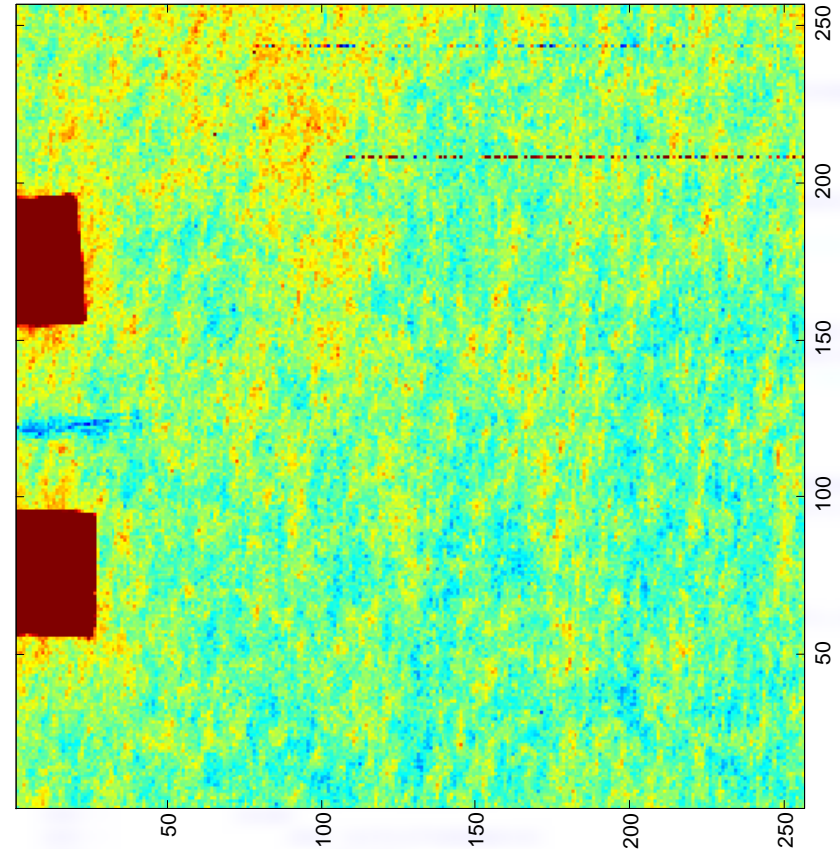
Loading equipment fixed on the loading stage.

X-ray device Medipix-2 with a $700\mu\text{m}$ thick Si sensor.
(behind the discs with calibration filters on right).

Magnification 3.6x

Radiographic visibility of inner material structure

- The radiographic observation of internal material structure is quite simple for materials like spongiosis bones, reinforced composites, cellular materials etc.
- Internal grainy structure of a metal becomes recognizable when the variations in chemical composition of individual grains are presented.
- Grainy structure features projected in radiogram have typically dimensions of tents microns.



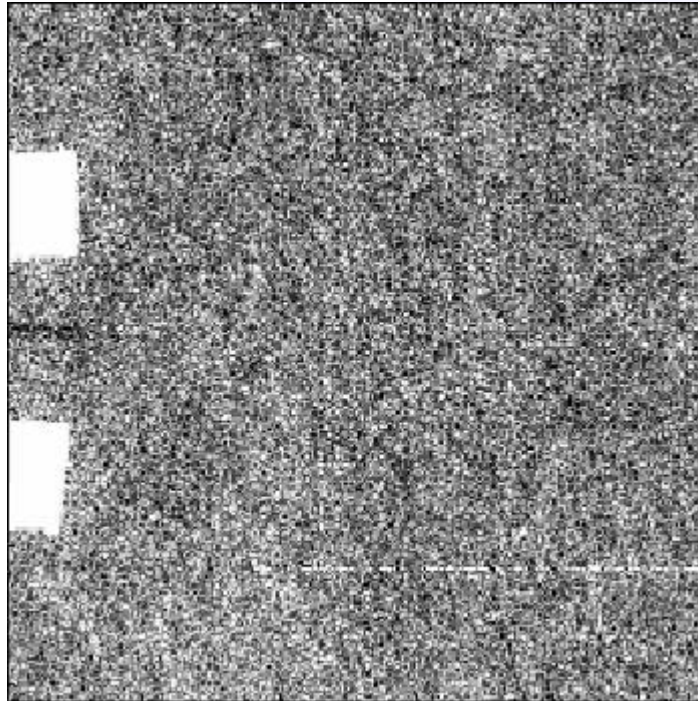
The red color represents the thickest material (the contrast lead marks), the blue color represents the thinnest place of the specimen (it is the crack in the middle between the lead marks).

The vertically oriented grainy structure formed by the heat rolling is visible.

Radiography movie of the loaded specimen

5mm thick Al-alloy specimen.

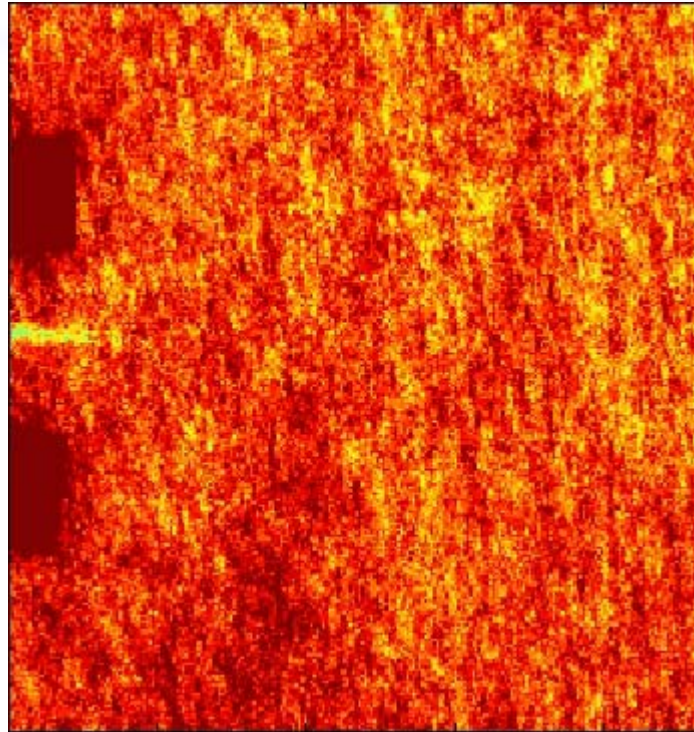
Continuous regime of the loading with the displacement velocity of 0.4mm/sec



The complete experiment took 34 min.

A radiographic snapshot with exposure time of 0.5 sec was taken each 0.85 sec (2420 images).

Floating average of the radiograms



The recognition of features within the sample is limited by the number of detected X-ray photons in each detector's pixel.

Therefore, a floating average of 40 snapshots was calculated (20 sec).

Generation of reference grid points

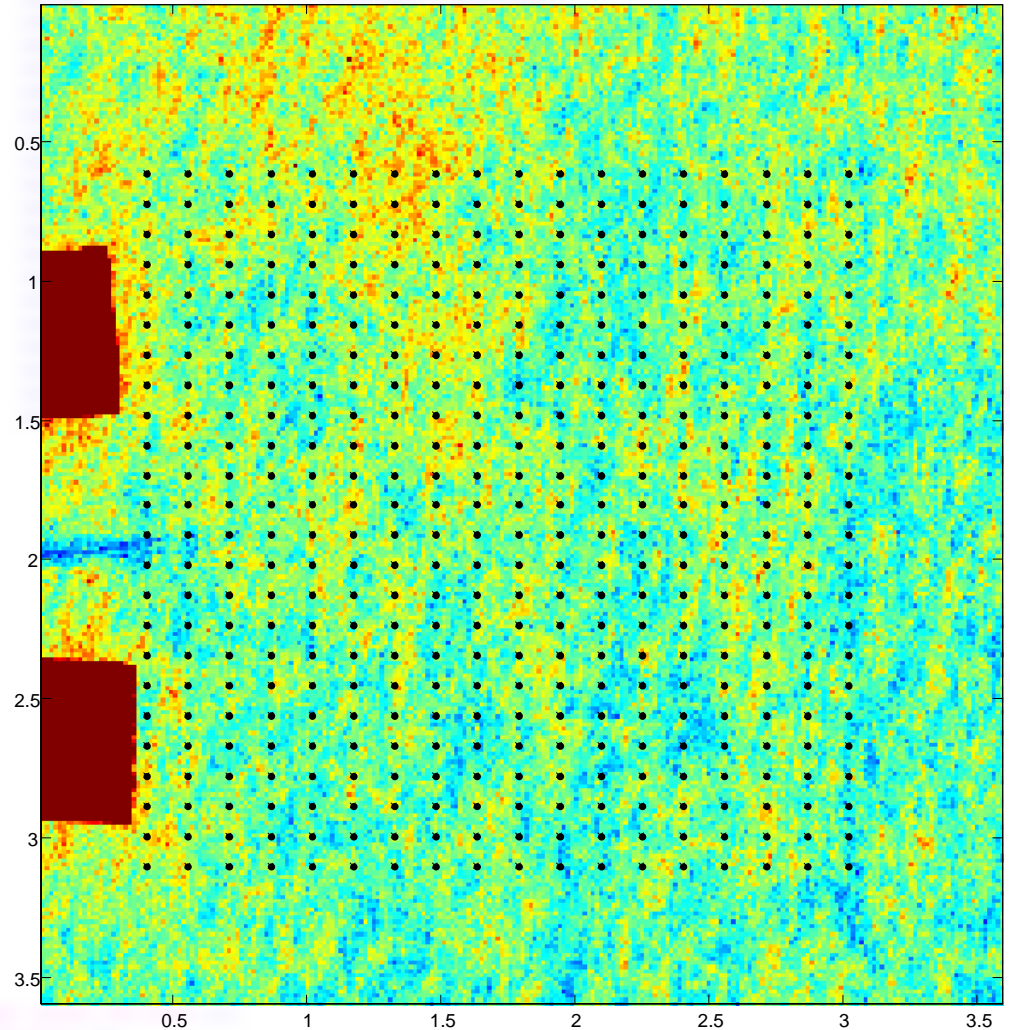
The grid of 432 **virtual** control points was generated based on the first image.

Reference subset was selected around each control point.

Subset has dimensions 25x25 pixels (0.39x0.39 mm)

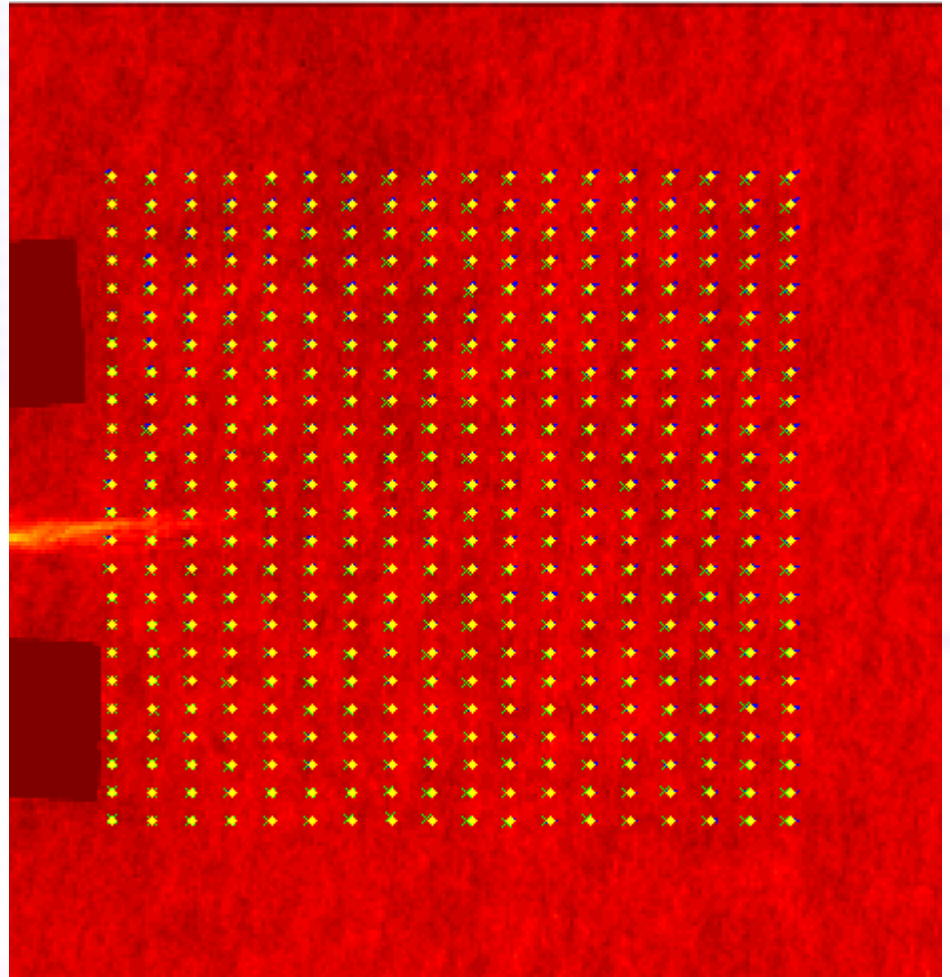
Grid pitch is 10/7 pixels (0.15/0.11 mm)

Tracks of the grid points were calculated over the all taken radiographs.



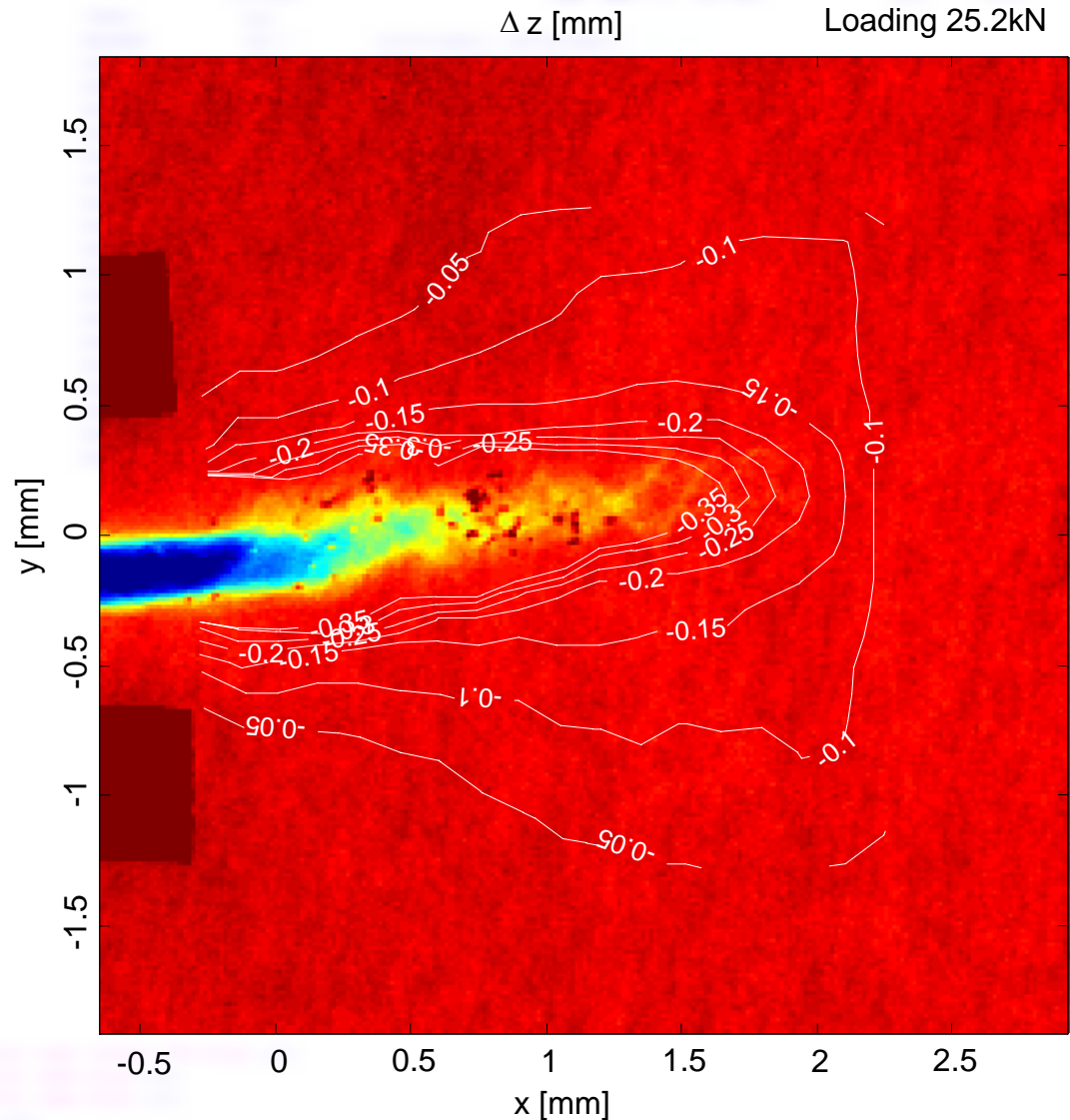
Virtual grid points tracking

- The yellow dot marks represent the initial positions, the blue line paths and the green “x” marks represent the final positions of the control points at the actual loading level.
- The white circle labels are used for control points where the correlation was lost at some loading level due to an intensive damage (the initial material structure was already significantly changed).

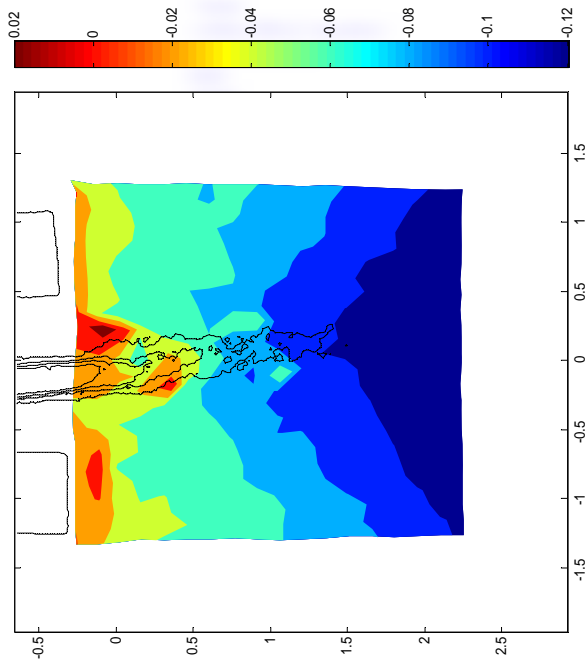


Out-of plane displacement

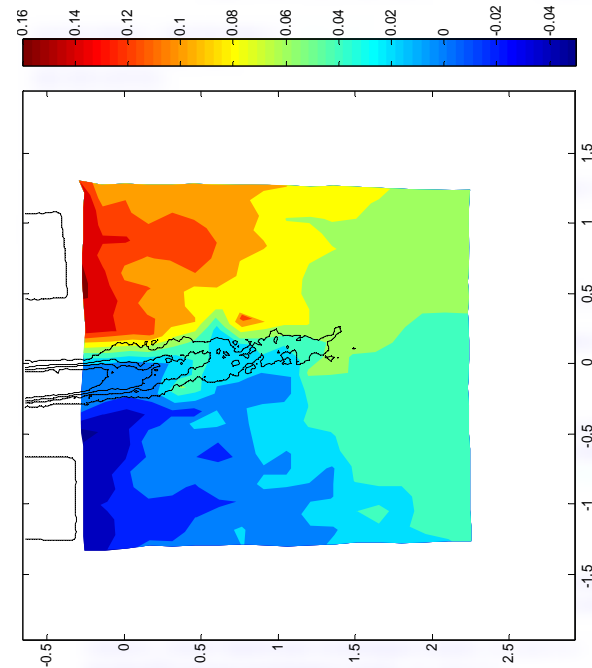
- The radiography of the specimen at maximal loading force of 22.5 kN with the Δz displacement field contoured by white isolines (mm scale).
- The fatigue crack tip has coordinates [0,0].
- Macroscopic crack has been observed in the next radiograms.



In-plane displacement fields



Displacement field Δx at max. loading force



Displacement field Δy .

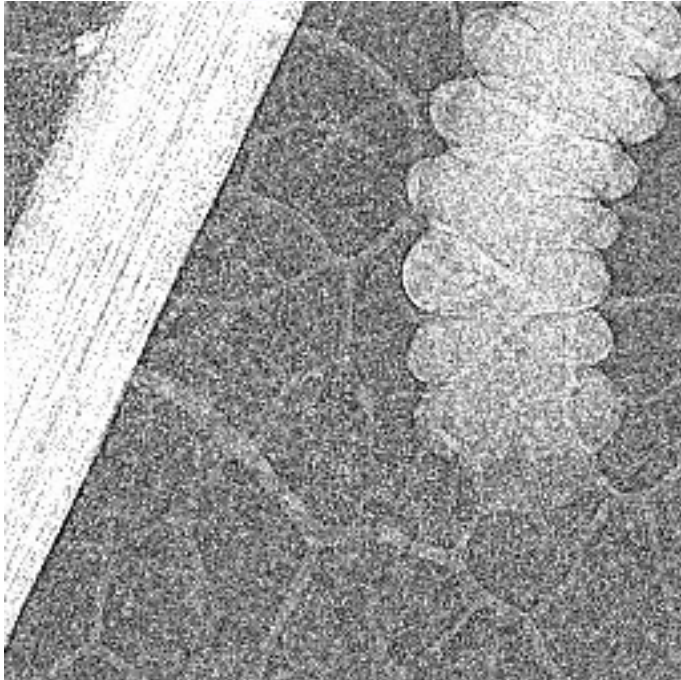
Both Δx (left) and Δy (right) displacement fields were calculated comparing the initial and actual positions of the control points.

The led marks and the damage zone are contoured by black hair lines.

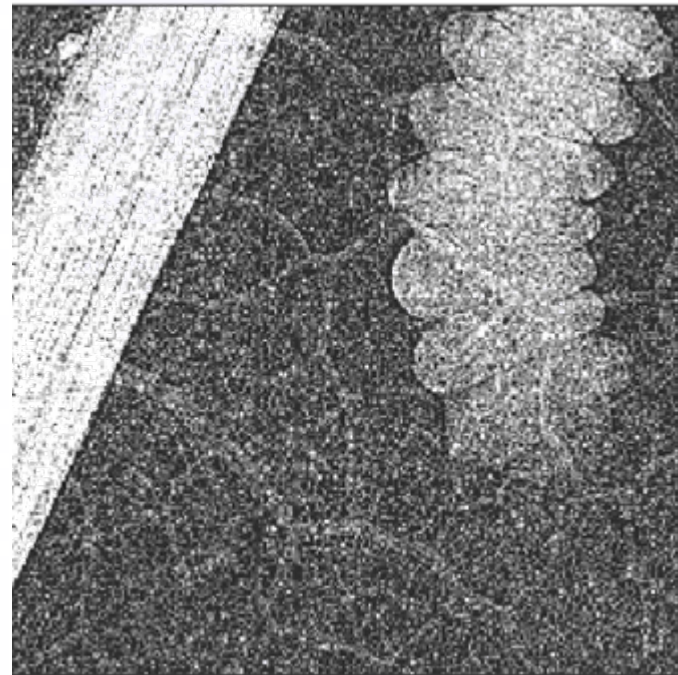
There is evidence of the highest gradient in Δy displacement around the indicated damaged zone.

**In vivo radiographic observation of the
Leaf miner (*Cameraria ohridella*)
living within leaf tissue.**

Worm inside of the leaf



Movie



Single radiogram

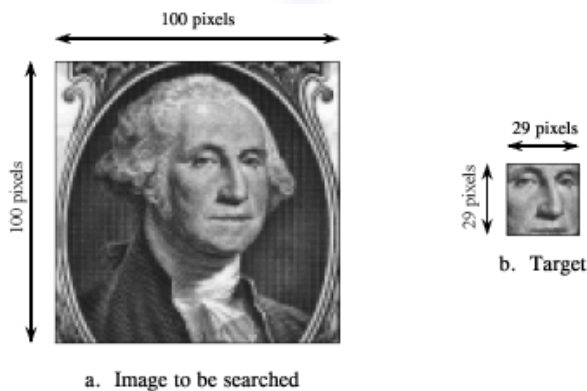
Single radiogram is quite noisy, moving is significant and chaotic.

DIC principles for significant increments of the displacement utilizing FFT

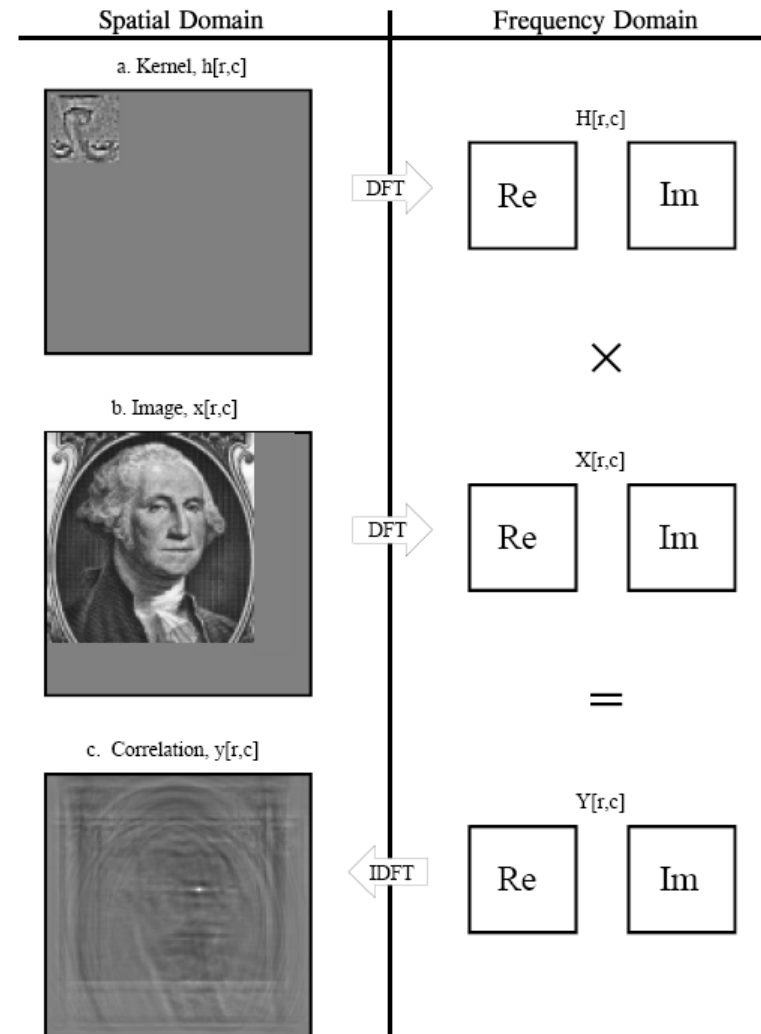
Target detection example.

The problem is to search the image of George Washington, (a), for the target pattern, (b), the face.

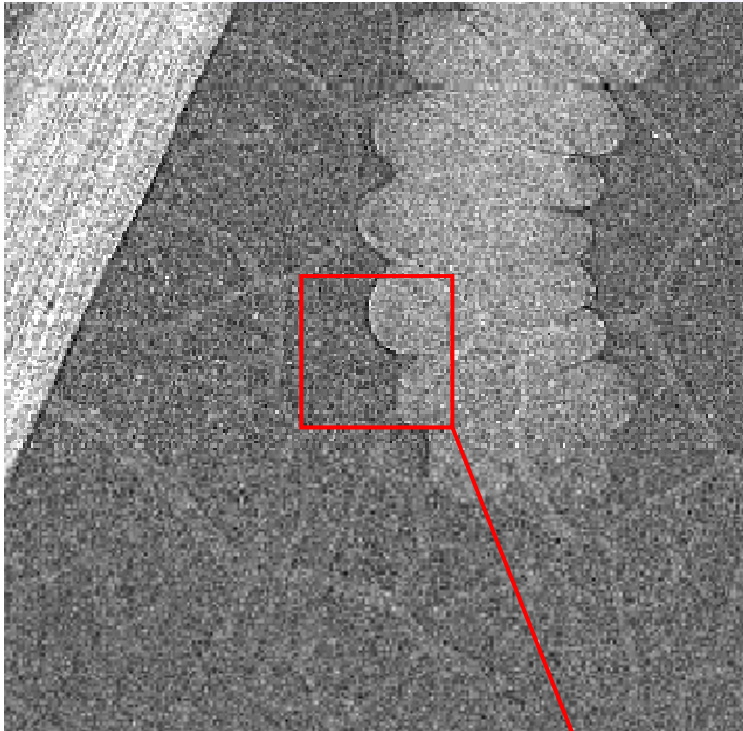
The optimal solution is *correlation*, which can be carried out by *convolution*.



- The images in (a) and (b) are transformed into the frequency domain by using the FFT.
- These two frequency spectra are multiplied, and the Inverse FFT is used to move back into the spatial domain.



Processing of the data

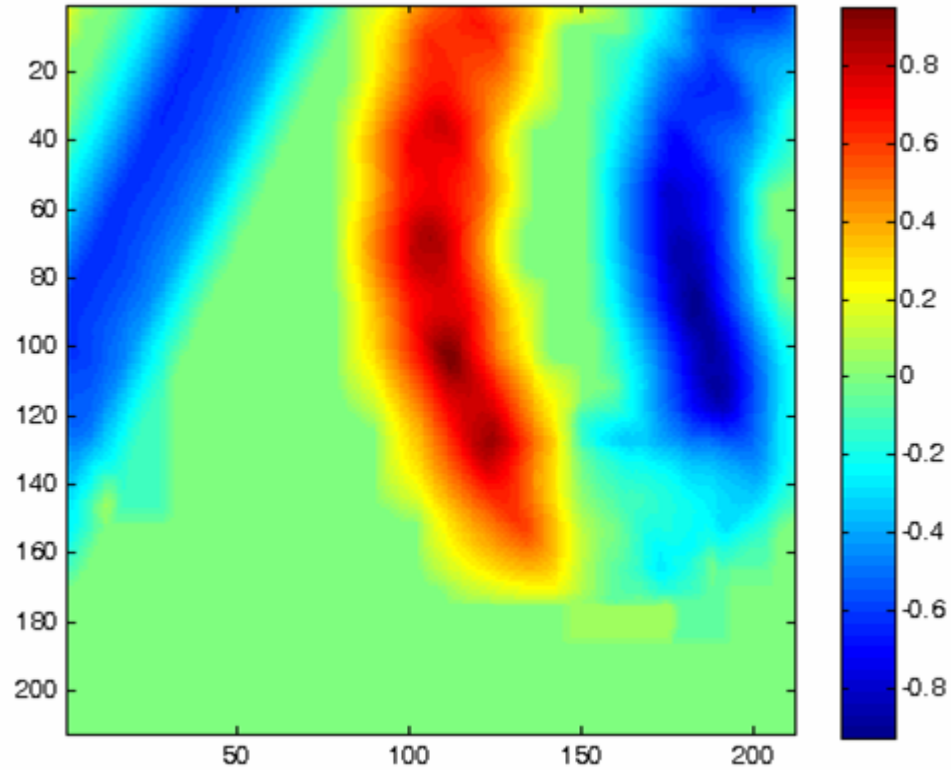


Region of the interest



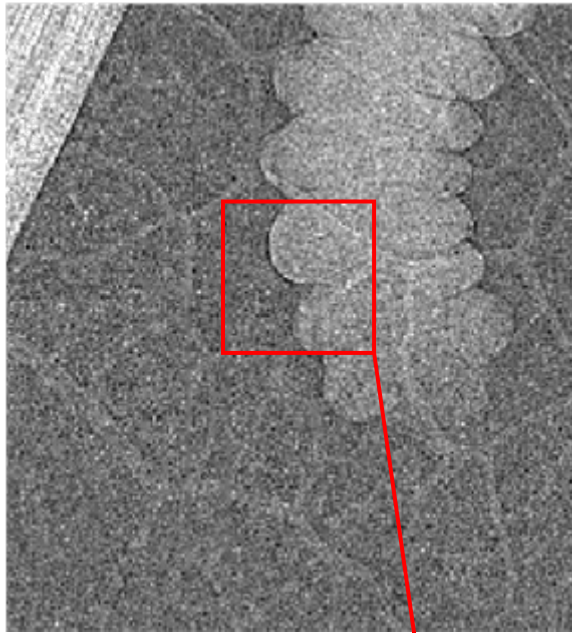
Lpf filter, averaging filter, binarization

Correlation map

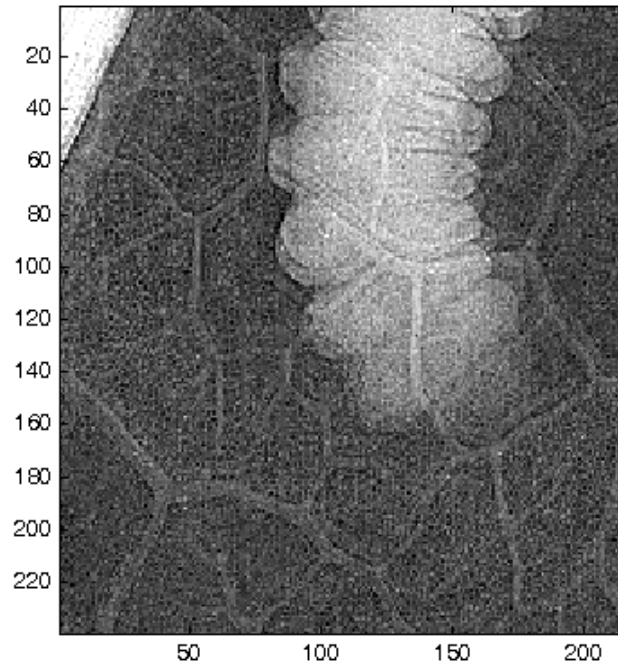


Summing of correlated images

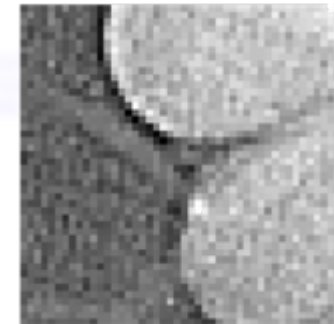
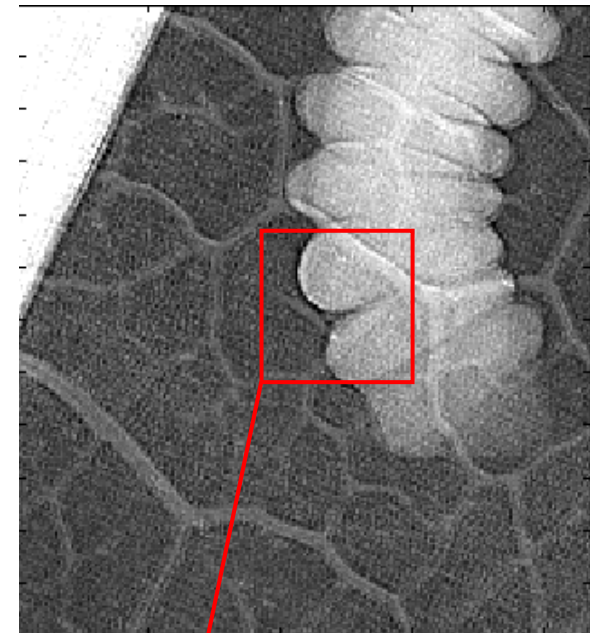
Single radiogram



45 radiograms summed.
Motion is not reflected.



45 radiograms summed.
Motion is reflected,



Conclusions

- The X-ray image correlation technique for increasing of radiographs quality was successfully realized.
- XDIC methodology is suitable for chaotic as well as for continuous non periodical movements.

Acknowledgement

This work has been supported in part by Research Grant No. 106/04/0567 of the Grant Agency of the Czech Republic and by the Ministry of Education, Youth and Sports of the Czech Republic under Research Project AV0Z20710524 and MSM6840770040.

Work carried out within the framework of the CERN Medipix Collaboration